Experimental demonstration of various approaches reducing the carbon footprint of RC members

Lazar Azdejkovic[1], Antroula Georgiou[1], Tamás Mészöly[1,*], Giorgio Mattarollo[1], Antonio Basso[2], Norbert Randl[1]

1. Department of Civil Engineering and Architecture, Carinthia University of Applied Sciences, Villach, Carinthia, Austria
2. Antonio Basso S.p.A., Treviso, Italy

*Corresponding author email: meszoely@cuas.at

Abstract

The article presents and examines strategies for reducing the greenhouse gas emissions of reinforced concrete structural elements, based on a series of large-scale beams tested under three-point bending as part of the Interreg research project SITAR. The study explores several material- and topology-related variables, aiming at improving the environmental performance of the structural members: the type of cement used (CEM I vs. CEM II), cross-sectional reduction through geometric optimisation, the use of UHPC, and finally the retrofit of a lower-capacity beam using TRC. All beams are designed to achieve similar bending capacity. The paper presents the results of the experimental programme, evaluates the Global Warming Potential (GWP) of the individual structural elements, and then compares and evaluates their load-bearing and environmental performance. A comparison of the GWP of the beams in terms of A1–A3 (cradle-to-gate) embodied carbon shows a 15% reduction achieved by changing only the type of cement. A 36% reduction is observed when geometry optimisation is added, while a similar 39% reduction is also achieved when the beam is optimised using UHPC. 78% reduction is achieved when retrofitting is applied to the existing beam. The results and conclusions of this study provide insights for more sustainable structural design strategies and contribute to the shift in mindset that is necessary to advance a more environmentally friendly construction industry.

Keywords: *Global Warming Potential (GWP), Sustainability, Textile-reinforced concrete (TRC), Ultra-high-performance concrete (UHPC), Material efficiency.*

1. Introduction

The construction sector is responsible for a substantial share of global greenhouse gas (GHG) emissions, with cement production alone accounting for approximately 7–8 % of worldwide anthropogenic CO_2 emissions (Aïtcin 2000; Scrivener, John and Gartner 2018). As reinforced concrete (RC) remains the most widely used construction material worldwide, reducing its embodied carbon has become a key objective in the transition towards a climate-neutral built environment. Commonly proposed mitigation strategies include the use of low-clinker and blended cements, the incorporation of industrial by-products and recycled aggregates, optimisation of structural geometry, and the application of high- and ultra-high-performance cementitious materials (Mehta and Monteiro 2014; Habert et al. 2020).

Within this context, the Interreg SITAR project (Supporting the construction Industry in the Transition towards climate-friendly practices in the Alpine Region) investigates innovative cementitious materials and strengthening solutions suitable for sustainable construction in the Alpine region. The project focuses on eco-concretes based on CEM II binders and industrial by-products, High-Performance Concrete (HPC), Ultra-High-Performance Fibre-Reinforced Concrete (UHPC), and Textile-Reinforced Concrete (TRC), with particular emphasis on the retrofitting of existing RC members. Fiber-reinforced high-performance cementitious materials offer clear mechanical and durability-related advantages compared to conventional concrete: increased strength, enhanced ductility, improved crack control, and extended service life, which in turn allow reductions in structural dimensions and overall material

consumption (Graybeal 2011; Habel and Gauvreau 2008; Brühwiler and Denarié 2013). Despite these advantages, the widespread application of high-performance cementitious materials in structural practice remains limited. One major barrier is the lack of harmonised design provisions and the fragmented treatment of advanced cementitious composites across existing standards and recommendations (fib 2013; CEN 2004; Hegger and Voss 2008; Triantafillou 2016).

Another challenge is the limited integration of structural and environmental considerations in current design frameworks. While numerous studies report material-level environmental indicators for concretes of varying strength classes or binder compositions (Flower and Sanjayan 2007; Damineli and John 2010; Van den Heede and De Belie 2016), far fewer investigations consider structurally equivalent elements, in which differences in geometry, reinforcement concept, and material efficiency are explicitly accounted for (Müller, Haist and Vogel 2014; Van den Heede and De Belie 2016). Moreover, functional equivalence is assumed rather than experimentally validated, and environmental comparisons are frequently decoupled from actual structural behaviour (Damgaard et al. 2016; Jayasinghe et al. 2020). As a result, partly contradicting conclusions are reported in the literature, with some studies indicating increased environmental burdens for high-performance concretes due to higher cement content, while others highlight their sustainability potential when reduced cross-sections and enhanced structural efficiency are considered (Müller, Haist and Vogel 2014; Damgaard et al. 2016). This limits the applicability of such results for practical design decisions, particularly when comparing new construction with strengthening and other retrofitting strategies for existing structures, where the increase of structural capacity plays a decisive role (Brühwiler and Denarié 2013; Zhang et al. 2024).

The present study addresses these gaps through a comparative experimental and analytical investigation of reinforced concrete beams designed to achieve approximately equal bending capacity. For each beam, the Global Warming Potential (GWP, cradle-to-gate life-cycle stages) is evaluated using an equivalent functional unit defined as one beam member of identical length and comparable structural capacity. By directly combining experimentally verified bending capacity with material-resolved environmental indicators, the study provides quantitative evidence of the sustainability gains achievable through material substitution, structural optimisation, and retrofitting instead of replacement.

2. Methodology

The methodological framework is based on comparative design of reinforced concrete beams that achieve similar target bending capacity while utilising different material compositions and geometric configurations. Four beams for new construction and one for retrofit were selected. The new beams include a reference RC beam produced with CEM I cement (B1), an eco-concrete beam incorporating CEM II binder and aggregates recycled from the steel industry waste (B2), a geometry-optimised I-section beam with the same eco-concrete (B3), and an UHPC beam designed according to Austrian UHPC guidelines (ÖBV 2023) (B4). Additionally, a substandard existing beam was strengthened using a textile reinforced concrete/mortar (TRC/TRM) system (B5) to investigate the effectiveness of strengthening relative to reconstruction.

The structural design of beams B1–B3 follows Eurocode 2 (CEN 2004) provisions for flexure and shear, using rectangular stress-block assumptions and standard partial safety factors. Reinforcement quantities were determined such that each beam achieves a bending capacity of approximately 240 kNm. The UHPC beam (B4) was designed using the Austrian UHPC guideline, which accounts for fibre-bridging effects, tensile softening behaviour, and material-specific strain limits. For the retrofit case (B5), sectional analysis was performed in accordance with CNR-DT 215/2018, incorporating the tensile behaviour of carbon textile reinforcement, the bond-dependent strength limits of the composite, and compatibility of strains between concrete, steel reinforcement, and TRC layers.

Environmental assessment was conducted by calculating the Global Warming Potential (GWP) at life-cycle stages A1–A3 according to EN 15978 for each beam. GWP results were expressed as total kg CO_2-eq per beam, as defined in Section 3.3, enabling direct comparison between alternative designs with equal load-bearing capacity. This methodology provides a consistent basis for evaluating the effectiveness of material substitution, cross-section optimisation, and the use of high-performance composites in reducing embodied carbon in structural concrete elements.

3. Experimental Programme

3.1. Scope and Assumptions

The experimental programme investigates the structural and environmental performance of five reinforced concrete beams designed or retrofitted to achieve an equivalent bending resistance of approximately 240 kNm. The purpose is to compare alternatives under a unified mechanical performance target. All beams share the same span, loading configuration, and support conditions. Material characterisation tests were carried out for each concrete type used, ensuring that the structural assessment and GWP estimation rely on actual measured properties, not nominal design values. The comparison is based on similar mechanical performance, while potential differences in service life and durability are outside the scope of this study. The study assumes that differences in construction processes, curing, and end-of-life do not significantly affect the comparative conclusions; therefore, the environmental study focuses on life-cycle stages A1–A3 only.

3.2. Input Parameters

The input parameters used in this study are based primarily on experimental material characterisation conducted on all mixes employed in the beam production. For each concrete type (CEM I, eco-concretes, and UHPC), standard tests were performed to determine compressive strength, apparent density, and, where applicable, tensile or flexural properties. These experimentally obtained values represent the actual material behaviour of the beams tested and are used to interpret the structural response. Embodied CO_2 values were taken from product-specific Environmental Product Declarations (EPDs), prioritising regional data for cement, aggregates, steel reinforcement, UHPC constituents, textiles, and mortar. Material quantities derived from beam fabrication were combined with these GWP factors.

3.3. Functional unit and derivation of embodied CO_2 intensity

The functional unit is defined as one beam capable of resisting a bending moment of 240 kNm under three-point bending, consistent with the mechanical target of the experimental program. This ensures that all environmental comparisons are made on the basis of equivalent structural performance, avoiding distortions arising from differences in strength or geometry.

The embodied CO_2 intensity for each beam (A1–A3) was calculated by multiplying the quantity of each material component – concrete volume, steel reinforcement mass, UHPC volume, textile area, and mortar volume – by the corresponding GWP values from manufacturer EPDs. The total environmental impact is expressed as kg CO_2-eq per beam, enabling direct comparison of material substitution, cross-section optimisation, and strengthening strategies.

$$CO_{2beam} = V_c \cdot GWP_c + m_s \cdot GWP_s \quad (1)$$

where V_c is the concrete volume per meter of beam, GWP_c is the embodied CO_2 emission factor of concrete (kg $CO_{2\text{-eq}}/m^3$), m_s is the mass of reinforcing steel per meter of beam, and GWP_s is the embodied CO_2 emission factor of reinforcing steel (kg $CO_{2\text{-eq}}$/kg). For the retrofitted beam, the embodied CO_2 is calculated solely from the materials added during the TRC intervention, as the objective is to compare this strengthening scenario against the alternative of demolition and full reconstruction represented by the new-build beam cases.

4. Materials and methods

4.1. Concrete, Reinforcement, and Composite Materials

For the construction of the new structural elements, two concrete mixes Normal Concrete (NC - CEMI) and ECO-concrete (CEM II) and one ultra-high-performance concrete mix (UHPC) were used. Beams B1, B2, B3, and B5 were cast at the "Antonio Basso" prefabrication plant in Italy using conventional (B1, B5) or eco-concrete (B2, B3) formulations developed within the SITAR project, with the mix designs shown in Table 1. All of these beams were reinforced with B450 C steel, the standard

reinforcement class widely used in Italy due to its high ductility and favourable mechanical properties. In contrast, the UHPC beam (B4) with UHPC as per Table 1, produced at the CUAS laboratory, was reinforced with B550 B steel, which is the commonly used reinforcement grade in Austria. Beam B5, designed as a substandard reference for retrofit evaluation, shared the same concrete mix as B1 but contained reduced longitudinal reinforcement, resulting in a lower bending capacity prior to strengthening. This beam was subsequently retrofitted at CUAS using a Textile Reinforced Concrete (TRC) system consisting of a commercially available, ready-to-use mortar (0–5 mm particle size) and a coated carbon textile. The textile consisted of a bidirectional grid with a mass of 284 g/m², equally distributed in both orthogonal directions, and a fibre-roving spacing of 25 mm. These properties ensured adequate tensile contribution and bond performance for the strengthening application.

Table 1. Concrete mixes used in casting B1, B2, B3, B4 and B5 specimen

Type	Material	NC [kg/m³]	ECO [kg/m³]	Material	UHPC [kg/m³]
Cement	CEM I Alpacem I 52.5R	370	-	CEM II/A-S 42.5R WT 27 C3A-frei Alpacem Austria	852.52
	CEM II Alpacem I 42.5R	-	340	Silica Fume (0.1–0.3 µm)	144.43
Filler	Dolomite filler ECO 0/100	80	110	Quartz powder (0.1–0.3 mm)	247.45
Aggregates	Crushed sand (0–4 mm)	980	980	Quartz sand (0.1–0.4 mm)	873.67
	Standard gravel (4–15 mm)	980	350	-	-
	Steel slag aggregates (4 8 mm)	-	310	-	-
	Steel slag recycled aggregates (8-16 mm)	-	320	Steel fibres 1%vol (0.15/10 mm)	78.5
S/P	Polycarboxylate-based superplasticizer	3.15	3.15	S/P	20.2
Water	Recycled water 100%	150	160	Water	196.95

4.2. Material Characterization

Complementary material tests were performed on all concrete batches and composite materials to determine the actual mechanical properties at the time of beam testing. For each concrete type (CEM I, eco-concretes, and UHPC), standard tests were conducted to quantify compressive strength, tensile splitting strength, density, and, where applicable, modulus of elasticity. For the TRC system, standard compressive and flexural mortar tests were carried out to characterize the matrix material, while the mechanical characteristics of the applied textile mesh were obtained from the technical datasheet provided by the manufacturer. These results are summarised in Table 2 and used to interpret the structural response of the beams. Compressive tests on cylinders and splitting tensile tests were performed in accordance with EN 206 and EN 12390-6:2023, respectively. The elastic modulus of the concrete was determined following EN 12390-13 at the same concrete age. For each type of test three specimens were tested. The flexural strength of the UHPC was determined in accordance to the ÖBV (2023), while the strength values of the TRC mortar were obtained by following EN196-1.

Table 2. Summary of mean mechanical properties of materials (standard deviations in parenthesis)

Material/Mix	$f_{cm,exp}$ (MPa)	$f_{ctm,sp}$ (MPa)	E_{cm} (GPa)	Density (kg/m³)	$f_{cfm,fl}$ (MPa)
Normal concrete	62.72 (6.42)	3.99 (0.77)	38.62 (0.89)	2420.79 (18.2)	-
Eco concrete	68.56 (0.49)	4.28 (0.32)	36.57 (2.62)	2584.71 (17.4)	-
UHPC	170.62 (2.32)	5.29 (0.35)	46.62 (0.71)	2380.35 (21.6)	13.46 (1.87)
TRC mortar	48.73 (1.84)	-	20.0*	2200.0*	5.45 (0.30)

*Values taken from the technical datasheet

4.3. Beam Geometry and Design

All beams were designed with a total length of 3.5m. Reinforcement layouts for B1–B4 followed the design configurations ensuring a target bending resistance of 240 kNm. B5 shared the same geometry and concrete as B1 but contained a smaller amount of longitudinal reinforcement, consistent with its

role as an existing "substandard" beam for retrofit evaluation. All beams, including B5, were detailed with adequate shear reinforcement to ensure flexural failure modes during testing. For B3 and B4, an optimised I-section geometry was adopted to reduce concrete volume. Prior to performing the retrofitting of the beam B5 the concrete surface was roughened, cleaned, and prepared, after which the TRC layers were applied manually. Mortar was placed in multiple passes to ensure proper embedding of the textiles. In order to encounter early debonding, bonded anchors were in addition positioned close to the ends of the strengthening layer. Such type of improved end anchorage had already been successfully tested in a foregoing project (Rossi et al 2021 a, b).

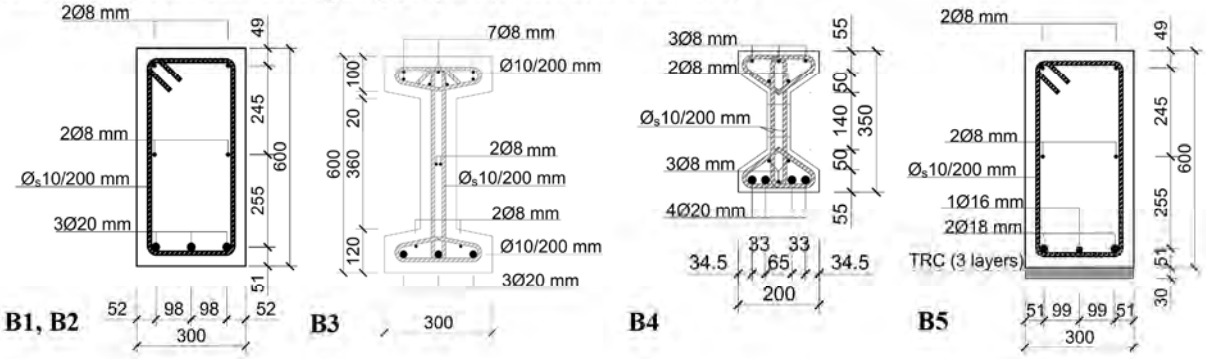


Figure 1. Cross-sectional geometry and reinforcement for each beam

4.4. Test Setup and Instrumentation

All beams were tested under three-point bending with identical support spacing and loading configuration. The metallic roller supports were spaced at 3000 mm, while the load was introduced at the top surface of the mid-span thus, a symmetric shear span of 1500 mm was achieved. Loading was applied under displacement control with a rate of 1 mm/min, using a servo-hydraulic actuator (max capacity of 2100 kN). The load–deflection response was continuously recorded until failure. Three LVDT's were placed on one side of the beam to measure the displacements at mid-span and supports (Fig. 2). Simultaneously, the deformations were tracked on the other side of the beam with a digital image correlation (DIC) system. For the latter, a set of four cameras were positioned 1.8 m from the beam surface so that the deformations of the 2000 mm wide middle area of the beam are obtained at the frequency of 1 Hz. The applied vertical load was directly logged from the loadcell.



Figure 2. Three point bending test setup

4.5. Environmental Data Acquisition

Material quantities from beam fabrication—including concrete, reinforcement, UHPC constituents, textile layers, and mortar—were combined with product-specific Environmental Product Declarations (EPDs) and manufacturer data consistent with EN 15804 to calculate embodied CO_2 emissions (A1–A3). For the concretes cast at the "Antonio Basso" precast factory, the emission factors used include 0.71 $kgCO_2/kg$ for CEM I, 0.60 $kgCO_2/kg$ for CEM II/A-LL, and for the UHPC cast at CUAS 0.47 $kgCO_2/kg$ for CEM II/A-S. Natural aggregates were assigned 0.00776 $kgCO_2/kg$, while the

recycled steel slag (by-product) aggregates ("Pittini granella") were assigned 0.00984 $kgCO_2/kg$. The high-range water-reducing admixtures were taken as 1.53 $kgCO_2/kg$ for Glenium ACE 440 and 1.53 $kgCO_2/kg$ for Sika ViscoCrete-20 Gold.

For UHPC, emission factors included microsilica (0 $kgCO_2/kg$ as a by-product), quartz powder (0.0234 $kgCO_2/kg$), quartz sand (0.0031 $kgCO_2/kg$), steel fibres (2.68 $kgCO_2/kg$), and water (0.0005 $kgCO_2/kg$). The TRC system used in beam B5 was evaluated using EPD-based values of 8.47 $kgCO_2/m^2$ per textile layer and 0.488 $kgCO_2/kg$ for the mortar. These emission factors were applied to the measured material quantities of each beam to determine the total embodied CO_2 per structural unit. For the retrofitted beam (B5), only the additional TRC materials were included, enabling a consistent comparison between strengthening and the alternative of demolition and reconstruction.

5. Results

5.1. Mechanical Performance

The load–mid-span displacement responses obtained from the three-point bending tests are shown in Figure 3. All specimens exhibit an initial linear elastic behaviour up to first cracking, followed by a reduction in stiffness associated with yielding of the longitudinal reinforcement. No premature shear failures occurred, confirming that stirrup detailing was adequate. The reference beam B1 reaches first cracking at approximately 160 kN, while the eco-concrete beams B2 and B3 show comparable cracking loads, ranging between 135 and 150 kN. After cracking, specimens B1–B3 display similar stiffness levels and a stable load increase up to reinforcement yielding. The optimised I-shaped beam B3 attains a peak sustained load comparable to or slightly higher than that of the prismatic reference beams, despite its reduced cross-sectional area, indicating an efficient utilisation of material under bending.

Distinct post-cracking behaviours are observed for the high-performance material solutions. Specimen B4 (UHPC) shows a significantly lower first-crack load but maintains a stable load-carrying capacity over a wide displacement range, with a relatively flat post-peak response, reflecting a progressive cracking process. In contrast, the textile-reinforced concrete strengthened beam B5 exhibits the highest peak sustained load among all specimens, exceeding 550 kN, together with increased post-cracking stiffness compared to the "new" beams. The TRC of B5 fails in a brittle manner at a ductility of 2.5 due to debonding at the anchorage end, yet the beam continues to display deflection ductility at a lower load level due to the existing steel reinforcement. Specimens were unloaded after sustaining the maximum load and the extensive reinforcement plastic deformation.

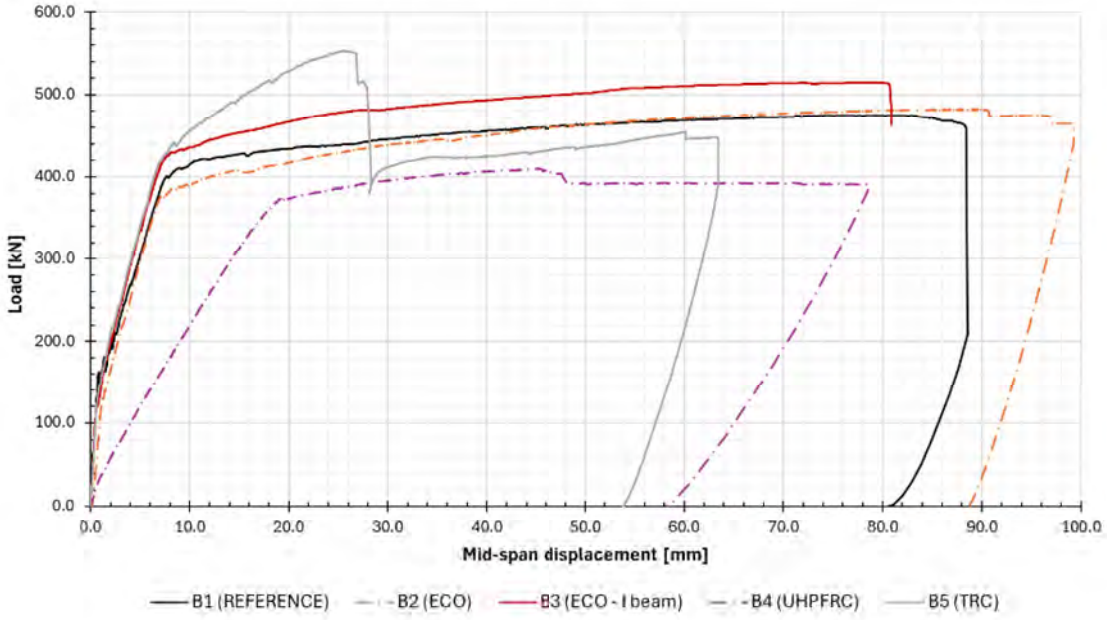


Figure 3. Load-deflection diagrams obtained in three-point bending tests

Table 3. Three-point bending test results outcomes

Specimen	first crack occurrence		reinforcement yielding		peak sustained load		failure mode
	disp. (mm)	load (kN)	disp. (mm)	load (kN)	load (kN)	M_{rd} (kNm)	
B1 (REF.)	1.08	159.60	8.05	401.30	475.25	356.44	Bending
B2 (ECO)	1.37	134.05	7.02	375.74	482.44	361.83	Bending
B3 (ECO)	0.72	122.16	7.83	426.51	514.44	385.83	Bending
B4 (UHPC)	1.00	26.07	19.20	374.03	410.00	307.50	Bending
B5 (TRC)	1.01	148.67	7.59	419.16	552.78	414.59	TRC anchor.

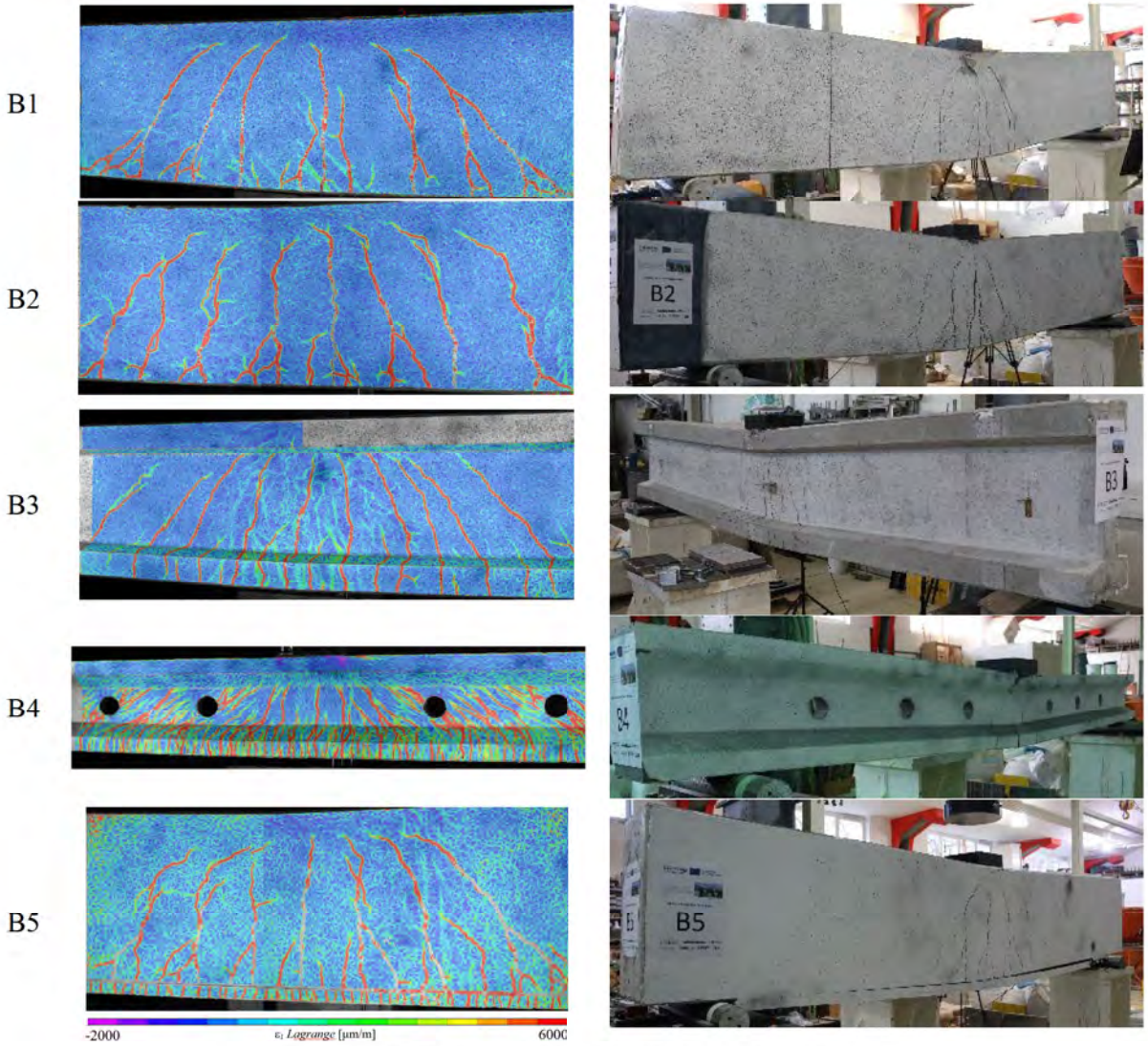


Figure 4. Crack patterns at yielding (left) and failure (right)

The crack patterns observed at yielding and at failure are shown in Figure 4. For specimens B1, B2, and B3, flexural cracks initiate at the tensile face beneath the loading point and propagate vertically with increasing load. As loading progresses, cracking localises in the mid-span region, leading to the formation of one dominant flexural crack at failure, accompanied by widening crack openings and concrete crushing in the compression zone. The observed behaviour indicates flexure-governed failure following yielding of the longitudinal reinforcement. The crack patterns observed in the five beams show clear differences related to material choice and structural configuration. The reference beam B1 exhibited a typical RC response with well-distributed vertical flexural cracks and significant widening near failure. The eco-concrete beam B2 showed a slightly higher crack density but comparable crack widths, confirming similar structural behaviour to CEM I concrete. The cracking density further

increased in the geometry-optimised beam B3, with the cracks concentrated primarily in the web, producing a fan-shaped distribution typical of slender web behaviour. The UHPC beam B4 developed numerous fine microcracks with very small widths, characteristic of strain-hardening and fibre-bridged tensile behaviour, leading to superior crack control. The TRC-strengthened beam B5 demonstrated markedly improved crack distribution compared to B1, with finer cracks forming mainly in the TRC layer, highlighting the effectiveness of the strengthening system in restoring and enhancing the flexural performance. Improved crack control of beam B4 and B5 may also contribute to enhanced durability and reduced maintenance demand.

5.2. Environmental Performance

To enable a consistent comparison of the environmental performance, all investigated solutions are evaluated using an equivalent functional unit, defined as one beam member of identical length and approximately equal structural capacity. This ensures that the reported differences in environmental impact are not influenced by variations in load-bearing performance. The environmental performance is quantified using the Global Warming Potential (GWP) for the life-cycle stages A1–A3 (cradle-to-gate), covering raw material extraction, transport, and product manufacturing. For beams B1–B3, the total GWP results from the combined contributions of conventional concrete and reinforcing steel. Beam B4 represents a steel-fibre-reinforced concrete solution; therefore, the reported concrete GWP value already includes the CO_2 emissions associated with the steel fibres. Beam B5 is a TRC reinforced beam, where the GWP consists of the fine-grained mortar and the carbon textile reinforcement. The effect of the local end anchorage was not considered as its impact decreases with the overall length of the TRC layer. The results for all demonstration beams are summarized in Table 4, while Figure 4 illustrates the material-resolved contributions to the total GWP per beam.

Table 4. GWP (A1–A3) per beam

Beam	Concrete [$kgCO_2$-eq/m^3]	V_c [m^3]	Steel [$kgCO_2$-eq/kg]	m_s [kg]	CO_{2beam} [$kgCO_2$-eq]
B1	283.05	0.63	0.764	71.2	**232.73**
B2	226.22	0.63	0.764	71.2	**196.97**
B3	226.22	0.364	0.764	87.3	**149.03**
B4	651.92	0.151	0.565	66.1	**135.56**
	Mortar [$kgCO_2$-eq/kg]	m_m [kg]	**Textile** [$kgCO_2$-eq/layer/m^2]	**3 layers** (A=0.3·2.5m^2)	
B5	0.488	58.05	8.47	2.61	**50.44**

Beam B1 serving as the reference solution exhibits the highest total GWP, amounting to 232.73 kg CO_2-eq per beam, with the dominant contribution originating from the concrete volume and a smaller share from reinforcing steel. By replacing conventional concrete with eco-concrete in B2, while maintaining identical geometry and reinforcement, the total GWP is reduced to 196.97 kg CO_2-eq, corresponding to a reduction of approximately 15 % compared to B1. This reduction is solely attributed to the lower emission intensity of the concrete material. In B3, the use of eco-concrete combined with a reduction of the concrete cross-section, results in a further decrease of the total GWP to 149.03 kg CO_2-eq, representing a reduction of approximately 36 % relative to the reference beam B1. Beam B4 which uses an alternative UHPC solution further minimizes the cross-section. The UHPC exhibits a higher GWP per cubic meter; however, the significantly reduced volume results in a total GWP of 135.56 kg CO_2-eq per beam. The total GWP of the retrofit solution B5 amounts to 50.44 kg CO_2-eq per beam, which is the lowest value among all investigated solutions and corresponds to a reduction of approximately 78 % compared to the reference beam B1.

The results indicate that reductions in global warming potential are primarily governed by material efficiency rather than material substitution. While the use of eco-concrete leads to measurable improvements, substantially larger reductions are achieved through cross-sectional optimization and structural system changes. The retrofit solution using textile-reinforced concrete exhibits the lowest environmental impact, demonstrating that preserving existing structural elements and adding only the

required capacity is markedly more effective than replacing the member with a newly constructed beam, even when advanced concrete technologies are employed.

Figure 5 combines the total cradle-to-gate global warming potential with the corresponding bending capacities of the investigated beams. Despite a substantial reduction in embodied CO_2 emissions from beams B1 to B4, the bending capacity remains within a comparable range, confirming that the applied material and geometric optimizations do not adversely affect structural performance. This indicates a progressive decoupling between environmental impact and load-bearing capacity, which becomes particularly pronounced for the optimized reinforced concrete and steel-fibre-reinforced solutions.

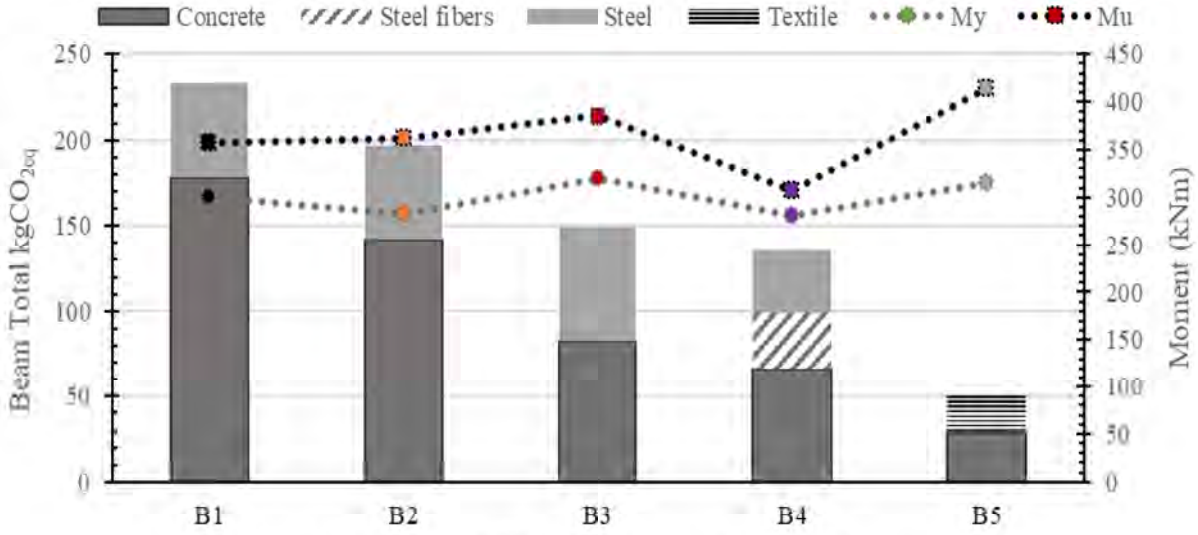


Figure 5. Comparison of $CO_{2\text{-eq}}$ emissions per beam and Moment capacity

The TRC-strengthened beam B5 exhibits the lowest GWP while providing the required structural capacity through a minimal material addition, highlighting the efficiency of retrofitting when compared to full replacement. The combined presentation of environmental and mechanical performance demonstrates that significant reductions in embodied carbon can be achieved without compromising structural capacity when material demand is minimized and existing structures are preserved.

6. Conclusions

This study assessed the mechanical and environmental performance of five reinforced concrete beams designed for comparable bending resistance. The tests showed that all specimens failed in flexure with no premature shear failure, confirming adequate shear reinforcement. Beams B1–B3 exhibited similar cracking and load–deflection behaviour, with B3 achieving slightly higher capacity despite reduced concrete volume. The UHPC beam (B4) displayed dense micro-cracking and a stable post-peak response, characteristic of fibre-bridged behaviour. The TRC-strengthened beam (B5) reached the highest peak load, with failure governed by local debonding at the textile anchorage.

The GWP assessment demonstrated that cement substitution alone (B1 → B2) leads to modest reductions (~15%), while combining eco-concrete with an optimised I-section (B3) reduces emissions by ~36%. Despite its higher per-volume footprint, UHPC (B4) reduced total GWP by ~42% due to its smaller cross-section. The most significant reduction was achieved by the TRC retrofit (B5), which required minimal additional material and resulted in ~78% lower embodied emissions compared to a newly cast reference beam. Overall, the results highlight that reductions in global warming potential are primarily governed by material efficiency rather than material substitution. Material efficiency, achieved through geometry optimisation, high-performance concretes, and especially retrofit strategies, offers substantially greater environmental benefits than material substitution alone. Retaining existing structural members and adding only the necessary strengthening proves to be the most effective pathway for reducing embodied carbon while maintaining required structural performance.

Acknowledgements

This work was conducted within the Interreg Italy-Austria Project "SITAR" – Supporting the construction Industry in Transitioning towards climate-friendly practices in the Alpine Region project. The authors acknowledge financial support from the European Regional Development Fund (Interreg VI-A Italy–Austria 2021–2027, Project ITAT-11-028) and the Carinthian Economic Promotion Fund (KWF).

References

Aïtcin, P.-C. (2000). Cements of yesterday and today: Concrete of tomorrow. Cement and Concrete Research, 30 (9), 1349–1359.

Brühwiler, E., and Denarié, E. (2013). Rehabilitation of concrete structures using ultra-high performance fibre reinforced concrete. Structural Engineering International, 23 (4), 450–457.

CEN (European Committee for Standardization). (2004). EN 1992-1-1: Eurocode 2 – Design of concrete structures – Part 1-1: General rules and rules for buildings. Brussels.

CEN (European Committee for Standardization). (2011). EN 15978: Sustainability of construction works – Assessment of environmental performance of buildings – Calculation method. Brussels.

CEN (European Committee for Standardization). (2016). EN 196-1: Methods of testing cement-Part 1: Determination of strength. Brussels.

CEN (European Committee for Standardization). (2021). EN 206: Concrete — Specification, performance, production and conformity. Brussels.

CEN (European Committee for Standardization). (2023). EN 12390-6: Testing hardened concrete — Part 6: Tensile splitting strength of test specimens. Brussels.

CEN (European Committee for Standardization). (2019). EN 12390-13: Testing hardened concrete — Part 13: Determination of secant modulus of elasticity in compression. Brussels.

CNR (Consiglio Nazionale delle Ricerche). (2018). Istruzioni per la Progettazione, la Qualificazione ed il Controllo di Interventi di Consolidamento Statico mediante l'utilizzo di Compositi Fibrorinforzati a Matrice Inorganica (FRCM). CNR-DT 215/2018, Rome, Italy.

Damgaard, A., Larsen, A. W., Christensen, T. H., and Schmidt, J. H. (2016). Comparative life cycle assessment of concrete with supplementary cementitious materials. International Journal of Life Cycle Assessment, 21 (4), 504–515.

Damineli, B. L., and John, V. M. (2010). Developing low CO_2 concretes: Is clinker replacement sufficient? Cement and Concrete Composites, 32 (8), 593–600.

fib (2013). fib Model Code for Concrete Structures 2010. Fédération Internationale du Béton (fib), Lausanne, Switzerland.

Flower, D. J. M., and Sanjayan, J. G. (2007). Greenhouse gas emissions due to concrete manufacture. International Journal of Life Cycle Assessment, 12 (5), 282–288.

Graybeal, B. (2011). Ultra-High Performance Concrete. FHWA-HRT-11-038, Federal Highway Administration, Washington, DC.

Habel, K., and Gauvreau, P. (2008). Response of ultra-high performance fiber reinforced concrete (UHPFRC) to impact and static loading. Cement and Concrete Composites, 30 (10), 938–946.

Habert, G., Miller, S. A., John, V. M., Provis, J. L., Favier, A., Horvath, A., and Scrivener, K. (2020). Environmental impacts and decarbonization strategies in the cement and concrete industries. Nature Reviews Earth & Environment, 1, 559–573.

Hegger, J., and Voss, S. (2008). Investigations on the bearing behaviour and application potential of textile reinforced concrete. Engineering Structures, 30 (7), 2050–2056.

Jayasinghe, C., Waldmann, D., and Teutsch, M. (2020). Environmental assessment of high-performance concrete structures considering structural efficiency. Journal of Cleaner Production, 262, 121303.

Mehta, P. K., and Monteiro, P. J. M. (2014). Concrete: Microstructure, Properties, and Materials. 4th edition, McGraw-Hill Education, New York.

Müller, H. S., Haist, M., and Vogel, M. (2014). Assessment of the sustainability potential of concrete and concrete structures considering their lifecycle. Structural Concrete, 15 (3), 353–370.

ÖBV – Österreichische Bautechnik Vereinigung (2023). *Richtlinie "UHPC"*. Österreichische Bautechnik Vereinigung (ÖBV), Vienna, Austria.

Pagel Spezial-Beton (2024). Technisches Merkblatt UM02, UM20, UM50.

Rossi, E., Randl, N., Mészöly, T., and Harsányi, P. (2021). Effect of TRC and F/TRC Strengthening on the Cracking Behaviour of RC Beams in Bending. Materials, 14(17), 4863. https://doi.org/10.3390/ma14174863

Rossi E, Randl N, Mészöly T, and Harsányi P. (2021). Flexural Strengthening with Fiber-/Textile-Reinforced Concrete. ACI Structural Journal, 118, 97-107. https://doi.org/10.14359/51732647

Scrivener, K. L., John, V. M., and Gartner, E. M. (2018). Eco-efficient cements: Potential economically viable solutions for a low-CO_2 cement-based materials industry. Cement and Concrete Research, 114, 2–26.

Solidian (2018). Solidian GRID Q142/142-CCE-25. Technisches Datenblatt.

Triantafillou, T. C. (2016). Textile Fibre Composites in Civil Engineering. Woodhead Publishing, Cambridge.

Van den Heede, P., and De Belie, N. (2016). Environmental impact and life cycle assessment (LCA) of traditional and "green" concretes: Literature review and theoretical calculations. Cement and Concrete Composites, 34 (4), 431–442.

Zhang, Y., Brühwiler, E., Denarié, E., and Bastien-Masse, M. (2024). Sustainability assessment of UHPFRC strengthening solutions based on experimentally verified structural performance. Structural Concrete, 25 (1), 1–16.